THE ASTROPHYSICAL JOURNAL, 465:181–190, 1996 July 1

THE SOFT AND MEDIUM-ENERGY X-RAY VARIABILITY OF NGC 5548: A REANALYSIS OF *EXOSAT* OBSERVATIONS

G. TAGLIAFERRI
Osservatorio Astronomico di Brera, V. E. Bianchi 46, 22055 Merate (Lc), Italy; gtagliaf@merate.mi.astro.it
G. BAO[1] AND G. L. ISRAEL[2]
International School for Advanced Studies (SISSA), V. Beirut 2–4, 34013 Trieste, Italy; Bao.gang@avh.unit.no, gianluca@vega.sissa.it
L. STELLA[2,3]
Osservatorio Astronomico di Brera, V. E. Bianchi 46, 22055 Merate (Lc), Italy; stella@merate.mi.astro.it
AND
A. TREVES
International School for Advanced Studies (SISSA), V. Beirut 2–4, 34013 Trieste, Italy; treves@tsmi19.sissa.it
Received 1995 July 27; accepted 1996 January 31

ABSTRACT

We present a detailed cross-correlation (CCF) and power spectrum reanalysis of the X-ray light curves of the bright Seyfert 1 galaxy NGC 5548 obtained with *EXOSAT*. The 0.05–2 keV and 1–4 keV light curves are cross-correlated with the 1–9 keV and 4–9 keV light curves, respectively. We discuss how spurious time lags can be introduced by systematic effects related to detector swapping as well as the switching on and off of the instruments. We also find strong evidence that one of the ME detectors was not working normally during the second part of the 1986 March observation. When these effects are taken into account, the CCF peaks are in all cases consistent with the absence of delays between X-ray variations at different energies. This is unlike the results found by several authors based on the same data.

The power spectra of the 1–9 keV light curves are calculated, and a detailed search for quasi-periodic oscillations (QPOs) is carried out on these spectra by using a new technique for the detection of periodic (or quasi-periodic) signals even in the presence of source noise variability. No significant peaks are found above the 95% confidence detection threshold, except during the second part of the 1986 March observation, most probably as a consequence of the ME detector malfunctioning. We discuss and compare our results with those published by Papadakis & Lawrence in 1993.

Subject headings: galaxies: individual (NGC 5548) — galaxies: Seyfert — X-rays: galaxies

1. INTRODUCTION

NGC 5548 is a bright, close-by ($z = 0.017$) Seyfert 1 galaxy that was studied extensively in different bands of the electromagnetic spectrum. A large variability of both lines (optical–UV) and continuum have been reported, which makes the source an important laboratory for exploring the mechanisms of spectral formation in active galactic nuclei (AGNs). In particular, the study of correlations and time lags between the various spectral components represents an important technique for constraining the geometry of the emitting regions (see, e.g., Mushotzky, Done, & Pounds 1993 and references therein). From a systematic study of *IUE* spectra (1200–3000 Å; Clavel et al. 1991), a strong correlation between emission lines and continuum variability was established, with lines responding to the continuum variations with delays of 10–70 days, depending on the degree of ionization of the species (a higher ionization corresponds to a smaller delay). Systematic UV–X-ray observations indicated a strong correlation in the continuum variability in the two bands with an upper limit of ≤ 6 days to any delay (Clavel et al. 1992). This, together with the simultaneous optical UV continuum variations, showed that at least a component of the optical–UV continuum should be generated by reprocessing of the X-rays, rather than by the intrinsic disk variability, which should be characterized by longer timescales (Molendi, Maraschi, & Stella 1992). *ROSAT* observations of a soft X-ray flare with correlated variability in the UV, but without a corresponding change in higher energy X-rays (Done et al. 1995; Walter et al. 1995), made apparent the complexity of the processes occurring in the object. New simultaneous observations at various wavelengths are currently being analyzed (see, e.g., Korista et al. 1995 and references therein).

The importance of reprocessing on both cold and warm material is confirmed by the observation of a Fe K fluorescent line at a centroid energy of ~ 6.4 keV and of a Fe absorption edge at ~ 8 keV superimposed on a rather complex continuum (Nandra et al. 1991). This rich observational scenario may be accounted for by models in which a hot corona above the accretion disk provides the hard X-ray photons. At the same time, these photons are in part reprocessed by an accretion disk that in turn generates the photons for the Compton cooling of the electrons in the hot corona (see, e.g., Haardt & Maraschi 1993; Życki et al. 1994).

Because of its ~ 4 day orbital period, which allows long uninterrupted exposures, and its wide spectral range (0.05–10 keV), the *EXOSAT* satellite was particularly appropriate for studying variability and reprocessing in the X-ray band on timescales of tens of hours or less. For a systematic study

[1] Current address: Department of Physics and Astronomy, Georgia State University, Atlanta, GA 30303; Bao@chara.gsu.edu.
[2] Affiliated to the International Center for Relativistic Astrophysics.
[3] Current address: The Astronomical Observatory of Rome, Via dell'Osservatorio 2, 00040 Monteporzio Catone, Rome.

of the variability of Seyfert galaxies and QSOs contained in the *EXOSAT* database, we refer to Grandi et al. (1992) and Green, McHardy, & Lehto (1993).

NGC 5548 was observed with *EXOSAT* 12 times in 1984–1986 with a total exposure of ~200 hr. Flux variations up to a factor of 4 and 3 between the various observations and within each observation, respectively, were clearly seen. A detailed analysis of the *EXOSAT* light curves was performed by several authors. Variability on timescales of hours was studied by Kaastra & Barr (1989, hereafter KB), who searched for delays between variations in the soft (0.05–2 keV) and medium-energy (2–6 keV) X-ray light curves, suggesting that soft X-ray variations lead by ~4600 ± 1200 s. This result, if confirmed, would have profound theoretical implications, favoring models, such as those mentioned above, in which the medium-energy X-rays are produced by Compton scattering off the UV/soft X-ray photons by electrons in a hot corona. Walter & Courvoisier (1990) re-examined the same data by using a different analysis technique and substantially confirmed the results of KB.

Papadakis & Lawrence (1993a, hereafter PL) performed a power spectrum analysis of the *EXOSAT* ME light curves and reported the likely detection of quasi-periodic oscillations (QPOs) in five of eight observations. They suggested that the frequency (~2 mHz) of the QPOs increases with source intensity, whereas the fractional root mean square amplitude of variability decreases as the source brightens. Since this behavior is similar to that of, e.g., compact galactic X-ray binaries, PL suggest that intensity-correlated QPOs in NGC 5548 may also arise from instability or variability in an accretion disk around a massive black hole.

Because of the quality of the *EXOSAT* light curves and the importance of the physical inferences derived from them, we feel justified in presenting a new and independent analysis of relatively old data. This is done in light of some systematic uncertainties that may arise in the analysis of the *EXOSAT* light curves from relatively faint sources (such as most AGNs). These uncertainties are discussed in greater detail in a paper on the BL Lac object PKS 2155 − 304 (Tagliaferri et al. 1991, hereafter Paper I).

In § 2.1 we summarize the characteristics of the *EXOSAT* light curves of NGC 5548. Our cross-correlation (CCF) analysis for different X-ray energy bands is described in § 2.2. Details on our search for QPOs are given in § 2.3. The conclusions are in § 3.

2. DATA ANALYSIS

2.1. *Light Curves*

The data considered here have been obtained through the *EXOSAT* database and refer to the low-energy imaging telescope (LE) and the medium-energy experiment (ME) (White & Peacock 1988). The argon chambers of the ME experiment consisted of an array of eight collimated proportional counters mainly sensitive to 1–20 keV X-rays (Turner, Smith, & Zimmermann 1981). In order to monitor the background rates and spectrum, the ME was generally operated with half of the detector array pointed at the target and half at a nearby source-free region. The two halves were usually interchanged every 3–4 hr, a procedure described as *array swap* (hereafter *AS*). The LE telescope was used with a channel multiplier array (CMA) in the focal plane. The CMA was sensitive to the 0.05–2.0 keV energy band and had no intrinsic energy resolution (De Korte et al. 1981); however, a set of filters with different spectral transmission could be interposed in front of the detector.

The *EXOSAT* observations of NGC 5548 considered here are summarized in Table 1. Column (1) gives a letter identifying each observation; column (2) gives the observing date; column (3) gives the ME exposure time; column (4) gives the rms dispersion calculated from the 1–9 keV light curves with a binning time of 1000 s; column (5) gives the expected rms dispersion from counting statistics; column (6) gives the number of array swaps (*AS*); and column (7) gives the average 1–9 keV ME count rate (per ME array half). Columns (8)–(10) give the exposure times in the LE telescope used in conjunction with the aluminum/parylene (Al/P), boron (Bor), and thin-Lexan (3Lex) filters, respectively. The ME data products (energy spectra and light curves) stored in the *EXOSAT* database have been given a quality flag ranging from 0 (unusable) to 5 (excellent). Data with quality flags between 3 and 5 are of sufficiently good quality for a detailed analysis (see *The EXOSAT Database System: Available Databases* 1991). In our analysis we have considered all observations with the ME quality factor ≥3; this excludes two observations carried out in 1984 March and 1985 January (not listed in Table 1) with exposure times

TABLE 1

EXOSAT OBSERVATIONS OF NGC 5548[a]

Observation (1)	Date (yy/ddd) (2)	ME Exposure Time (s) (3)	Root Mean Squares Dispersion: From 1–9 keV Light Curves (counts s^{-1}) (4)	Root Mean Squares Dispersion: Expected from Count Statistics (counts s^{-1}) (5)	Number of Array Swaps (*AS*) (6)	ME Count Rate (counts s^{-1}) (7)	Exposure Times (s): Al/P (8)	Exposure Times (s): Bor (9)	Exposure Times (s): 3Lex (10)
A	84/032	17010	0.23	0.27	0	3.32 ± 0.18	1902	7153	3202
B	84/062	32630	0.26	0.20	0	4.44 ± 0.04	3483	3679	2763
C	84/193	59430	0.26	0.27	3	2.88 ± 0.03	11872	26488	11053
D	85/062	26800	0.22	0.20	1	3.65 ± 0.04	4434	11413	4605
E	85/159	25750	0.30	0.26	1	1.43 ± 0.05	6675	9915	3824
F	85/173	17020	0.30	0.20	2	3.03 ± 0.05	4252	6672	3311
G	85/186	23370	0.34	0.20	1	1.82 ± 0.04	3613	10963	3095
H	85/195	19020	0.22	0.19	1	1.35 ± 0.05	4040	...	2622
I	86/019	59860	0.39	0.22	3	4.97 ± 0.02	...	3469	39037
J	86/062	83830	0.45	0.29	6	3.82 ± 0.02	2392	4017	69809

[a] See text for a fuller explanation of columns.

of ~36,000 and ~22,000 s, respectively. An example of light curves is shown in Figure 1.

2.2. *Cross-Correlation Analysis*

In order to study the possible delays between the intensity variations in the various bands, we calculated the CCF of the LE (0.05–2 keV) and ME light curves (1–9 keV); this is indicated as LE/ME. For the LE, we considered only the light curves that were obtained with the 3Lex filter (which provided the highest photon throughput) and were longer than ~15,000 s. This allows us to search for delays longer than 1 hr. Observations I and J are the only ones suitable for the LE/ME analysis. We have also cross-correlated the 1–4 keV with the 4–9 keV ME light curves (ME/ME): this subdivision of the ME range for NGC 5548 provides comparable count rates in the two bands. The ME/ME CCF analysis was also performed for all the other observations given in Table 1. We used the standard CCF algorithm contained in the timing analysis package Xronos (Stella & Angelini 1992), which is well suited for equispaced and (nearly) continuous data, such as the *EXOSAT* light curves of NGC 5548.

In the analysis of the *EXOSAT* light curves of PKS 2155−304 (Paper I), we identified a number of systematic effects that may alter the CCF. These are briefly summarized here. A possible problem is related to the *AS* procedure, which leaves an uncertainty of up to ±0.5 counts s^{-1} in the level of the background subtraction. If the results of the CCF analysis change significantly by adding or subtracting one of the light curves across the *AS* with a constant value of up to 0.5 counts s^{-1}, then these results should be considered with caution.[4] Moreover, the presence of *AS* implies that the ME light curves are interrupted by gaps of a typical duration of 15 minutes. Although these durations are short compared to the total length of the entire light curves, the discontinuity that they introduce in the ME light curves can have strong effects on the CCF. To reduce the effects of the gaps, we fill them with the running average of the light curve calculated over a duration of ~1.5 hr. With this choice, the moving average follows the light curve behavior on timescales of hours, while the statistical fluctuations are reduced because of the relatively high number of points used in the average. For a given observation, the start and end times of the LE and ME light curves usually differ from a few minutes to tens of minutes. This can alter the shape of the CCF, especially if standard algorithms are used as in our case (see Paper I). To avoid the problem altogether, one should therefore make sure that the two light curves are strictly simultaneous, disregarding the data intervals in which only one light curve is available.

In our analysis we rebinned the light curves in time bins of 1000 s. We excluded all bins with an exposure time of less than 50%. In some cases we also used intensity windows in order to exclude those bins in the original light curves (resolution of 4–10 s) that were clearly affected by an inadequate background subtraction.

The CCF analysis of observation J, which is the longest and that for which KB report delays between soft and hard variations, was performed in two different ways for both the ME/LE and ME/ME cases. First, we considered the entire LE and ME light curves (see Fig. 1), with the gaps bridged with the running mean, and did not exclude the nonsimultaneous parts of the light curves. A ~6 hr interruption is apparent close to the beginning of the observation, which is due to the switch-off of the *EXOSAT* instruments at the perigee passage (see Fig. 1). If the ~1.5 hr long light curve interval that precedes this long gap is included in the analysis, than the LE/ME CCF shows a marked asymmetric peak centered on a delay of ~7000–8000 s (Fig. 2). If we exclude the gap or impose the simultaneity of the two light curves, then the delay is much shorter or not present at all. We note that the light curve shown in Figure 2 of KB not only includes the gap, but in the LE it includes another 30 ks of data at the end of the NGC 5548 observation, when this source was seen serendipitously in the field of the BL Lac object 1E 1415.6−2557 (Giommi et al. 1987). Of

[4] Because of a misprint, Paper I reports an uncertainty of up to ±0.05 counts s^{-1}; the correct value is the one reported here (Parmar & Izzo 1986; A. N. Parmar, private communication).

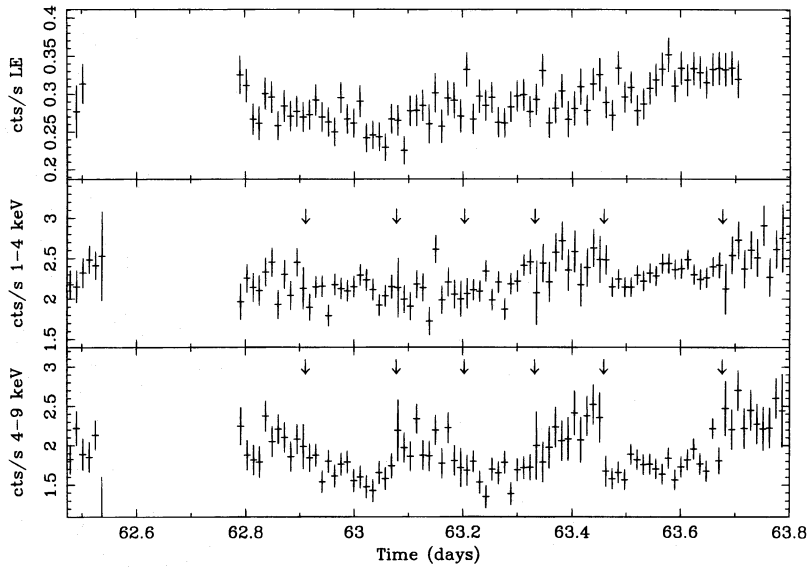

FIG. 1.—NGC 5548 LE (0.05–2 keV) and ME (1–4 and 4–9 keV) light curves during the longest *EXOSAT* observation (1986/062, observation J throughout the paper). The arrows show the array swaps of the ME detector halves; the corresponding data gaps of about 15 minutes are filled with the running mean (see text). Note the big gap at the beginning due to the switching off of the detectors at the satellite perigee passage and the lack of LE data at the end of the observation.

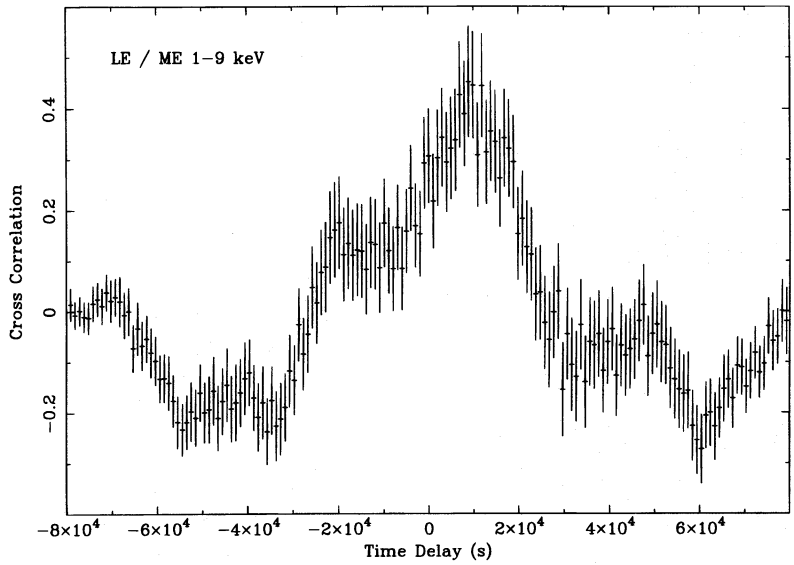

FIG. 2.—LE/ME light curve cross-correlations of observation J. All data shown in Fig. 1 have been used. Note that the peak centered on a delay of ~7–8 ks is also clearly asymmetric.

course, there are no ME data for this additional interval. It appears that for their timing analysis KB used all the data shown in their Figure 2, although this is not explicitly stated. As we have shown, the nonsimultaneity of the two data sets strongly affects the results of CCF analysis (see also Paper I). Therefore, we did not consider the extra LE data on NGC 5548 during the *EXOSAT* observation of 1E 1415.6−2557. Moreover, in all the rest of our analysis, we considered only strictly simultaneous data. We then also excluded the first ~7.5 hr from our analysis of the light curves of observation J. The LE/ME and ME/ME CCFs calculated in this way are shown in Figure 3. A peak is clearly present in the CCFs that is in both cases asymmetric and centered near zero time delay. To derive quantitative information on possible delays between the variations in the soft and hard X-ray light curves, we fitted the central peak of the CCF with a Gaussian function plus a constant. In the case of the ME/ME CCF, a linear term was added to the fit in order to account for the stronger asymmetry of the CCF (see Fig. 3). The results for centroid of the peak are +400 s (90% confidence interval: −800/+1500 s) and +1500 s (+500/+2700 s), respectively.

The second procedure consisted in dividing the light curve into three segments; the first two segments, about 6 and 7 hr long, contained only one array swap, and the third segment, about 11 hr long, contained two array swaps. The CCF was calculated for each segment. This treatment reduced the possible effects of the *AS* discontinuity on the CCF; however, it has the disadvantage of decreasing the longest detectable delay time (about 2–3 hr, a value still consistent with the delay time reported by KB). There is essentially no peak in the second interval for both the LE/ME and ME/ME CCFs, while in the first interval in both CCFs, there is a weak peak centered on zero time delay (Figs. 4*a*–4*d*). In the third segment, a clear peak is present in the ME/ME CCF, while a feature with a negative and a positive component can be noted in the LE/ME CCF (Figs. 4*e*–4*f*). This feature is due to the presence of the two array swaps; indeed, if we consider only one of the two array swaps each time, then the first array swap gives rise to only the negative peak, whereas the second array swap causes only the positive peak. Moreover, by looking at the ME light curves, it seems that the central parts (between the two array swaps; see Fig. 5) are not properly aligned with the other two. We tested how stable the CCF peaks are to

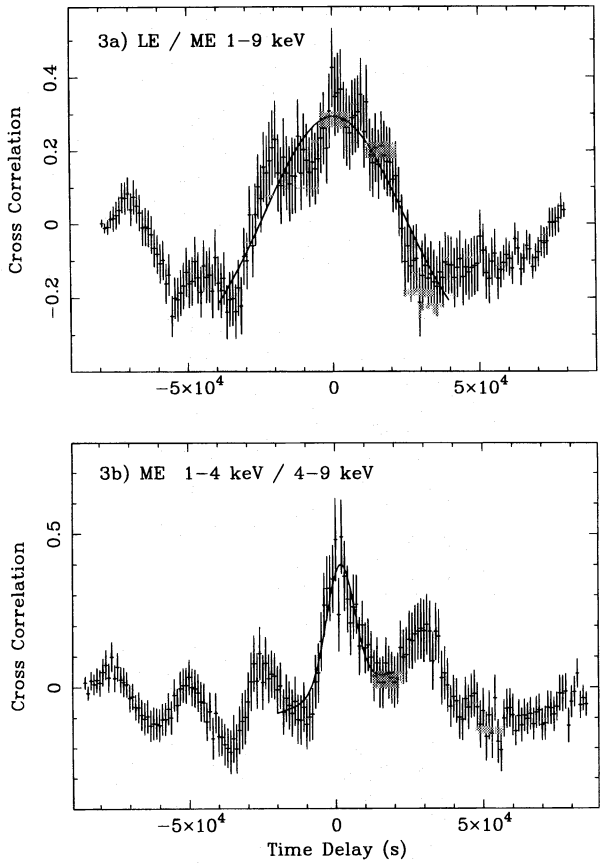

FIG. 3.—LE/ME (*a*) and ME/ME (*b*) light curve cross-correlations of observation J. A clear peak around zero time lag is clearly present in both cases. The Gaussian plus constant model fit to the central peak is also shown. The fit was carried out over a range of lags of ±40 ks and ±20 ks, respectively. In the ME/ME case, a linear term was added to the fit in order to account for the CCF asymmetry.

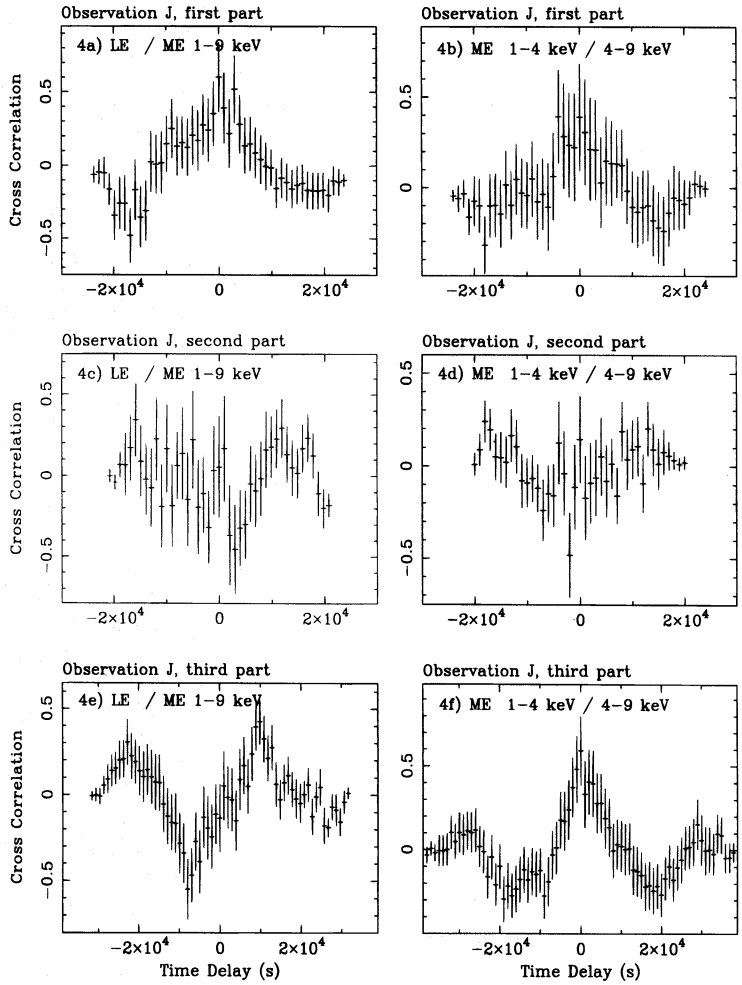

FIG. 4.—Cross-correlations of the light curves of observation J divided into three different segments (see text). A clear peak is present only in the third part (panels *e–f*).

the addition of a constant value to the central parts. For instance, in the ME/ME CCF, the peak disappears completely by adding 0.1 and 0.4 counts s^{-1} to the central 1–4 and 4–9 keV light curves, respectively (Figs. 5*a* and 5*b* show the two ME light curves before and after having added the above constant values to the central part). As a further test, we performed an LE/ME and an ME/ME CCF analysis by considering only the first 13 hr of this observation (i.e., three array swaps). Again, no peak is present in either CCF. We can conclude that the segmented analysis does not provide evidence for delays between the LE/ME and ME/ME variations.

Another problem emerged through a careful inspection of the ME light curves (Figs. 1 and 5). One can see that the light curve intervals between the fourth and fifth *AS* and after the sixth *AS* are much noisier than the others (this is seen even more clearly in light curves with a somewhat shorter binning time). This is probably due to one of the three aligned detectors (the first half of the ME in this case) not behaving normally. That this behavior arises from one of the detectors (and not from the source) is confirmed both by the lack of it in the LE light curve and by the fact that between the fifth and sixth array swap, when the relevant half of the ME array is offset, one of the detectors (detector B as reported in the ME Observation Log Book; A. Parmar, private communication) was switched off because of malfunctioning. After the sixth array swap, detector B was switched on again, but it was clearly not yet functioning properly (see Figs. 1 and 5). In this case the malfunctioning detector should be excluded from the analysis, something that was not done in the automatic analysis that generated the ME database products for this observation. We conclude that detector B in the first ME half is most likely responsible for the extra variability in the ME light curves. We intended to repeat the analysis starting from the ME raw data. However, we could not obtain the original data from ESA, since the relevant magnetic tape turned out to be unreadable (A. Parmar, private communication).

For all other observations in Table 1, because of the shorter exposure times and therefore lower number of array swaps (see Table 1), we considered the cross-correlation of the entire light curves with the data gaps bridged by the running mean. For observation I, the second longest, the LE/ME CCF is again flat, while the ME/ME CCF shows a strong peak centered on zero time delay (Fig. 6). It can be seen from the figure, however, that the *half-width at half-maximum* of this peak is comparable to the duration of the light curve segments between array swaps; this suggests that the peak might be due to the systematic uncertainties in the ME background subtraction across the array swaps. To test the reliability of this CCF peak we subtracted 0.2 counts s^{-1} from the first part of both ME (1–4 and 4–9 keV)

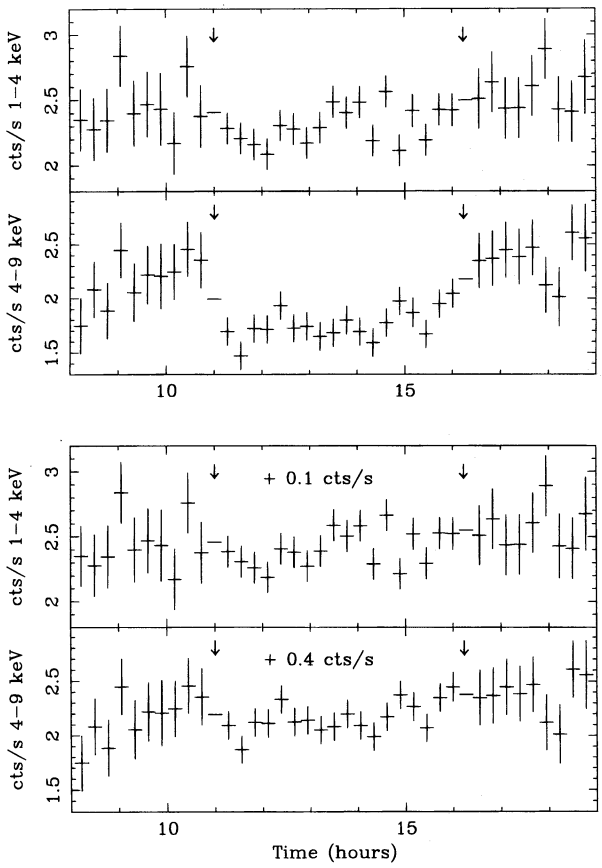

FIG. 5.—*Top:* Final part of the ME light curves of observation J; the arrows show the array swaps of the ME detector halves. Note the noisier light curves before and after the first and last array swap. *Bottom:* The same light curves after having added 0.1 and 0.4 counts s^{-1} to the central 1–4 and 4–9 keV light curves, respectively; the discontinuity due to the detector array swaps is clearly reduced.

light curves (before the first *AS*) and added 0.2 counts s^{-1} to the second and third parts of the 4–9 keV light curve, trying to reduce the discontinuity due to array swaps visible in the light curves. Again, this was sufficient to make the CCF peak disappear. Various other tests showed that by adding or subtracting 0.1–0.2 counts s^{-1} (which are well within the systematic uncertainties of the detector background subtraction) to selected segments of the ME light curves in between array swaps, the peak can become more pronounced or disappear altogether. The rms dispersion is clearly also affected by the array swaps; indeed, if we add 0.3 and 0.5 counts s^{-1} to the 1–9 keV light curve before the first and after the last *AS*, the resulting rms dispersion is 0.28 to be compared with the value of 0.39 given in Table 1.

For all other observations, we calculated only the ME/ME CCF. No peak was detected in the CCFs of observations A, C, D, E, F and H, consistent with the fact that no significant variability is present in the 1–9 keV light curves (see Table 1). Instead, a clear peak was detected in observations B and G (Figs. 7 and 8). In both cases, the peak is not centered on zero delay. This would indicate that the variations in the 1–4 keV light curves precede the variations in the 4–9 keV light curve by about 2000–3000 s. However, we also believe that these delays are spurious. In the case of observation G, the peak is almost certainly due to background subtraction uncertainties across the *AS*. Figure 9*a* gives the original ME light curves, while Figure 9*b* shows the same light curves after the addition of a constant value of 0.2 counts s^{-1} to the segments before the *AS*. The latter light curves show virtually no discontinuity across the *AS*, and the resulting CCF is flat. Again by adding 0.5 counts s^{-1} to the 1–9 keV light curve before the *AS*, the resulting rms dispersion is 0.18 to be compared with 0.34 of Table 1. We also used observation G to test whether the abrupt discontinuity introduced by the *AS* can cause the asymmetry seen in some of our CCFs. For instance, the CCF peak in Figure 8 is steeper on the right-hand side. If we subtract a constant from both ME light curves before the *AS* (increasing the *AS* discontinuity; see Fig. 9*a*), the peak asymmetry becomes more pronounced. Instead, by subtracting 0.5 counts s^{-1} from both ME light curves *after* the *AS* (changing the discontinuity from a step-up to a step-down), then an asymmetric peak, which is steeper on the left-hand side, is obtained. This clearly shows that the discontinuities introduced by the *AS* procedure can also make the shape of the CCF peak asymmetric. For observation B, which has no *AS*, the peak is probably due to instability in

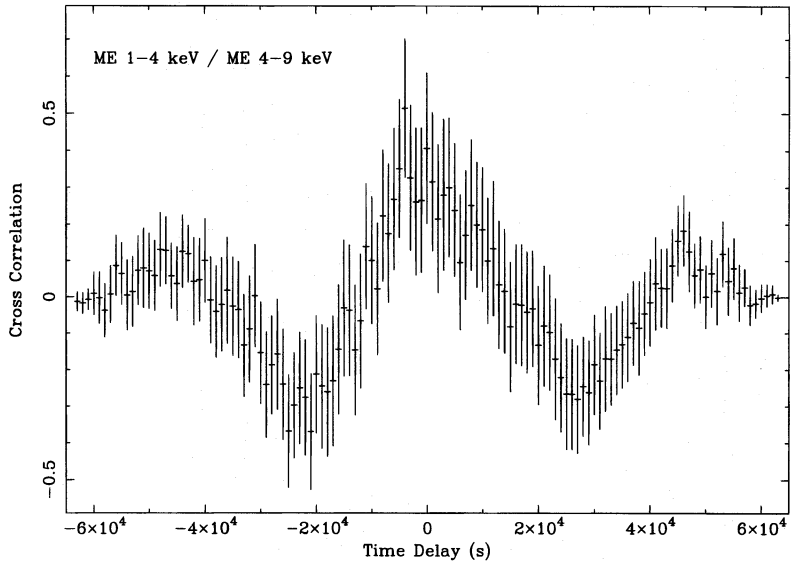

FIG. 6.—Cross-correlations of the ME light curves of observation I. Again, a strong peak centered on zero delay is clearly present.

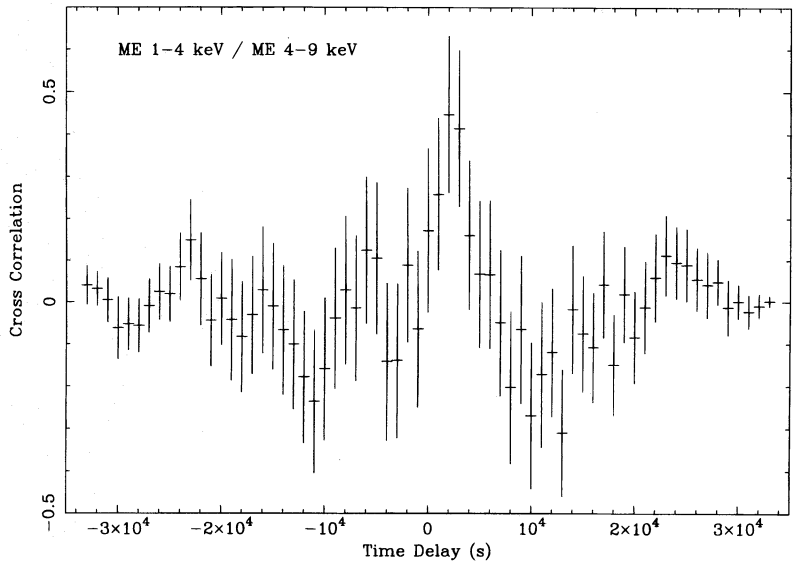

FIG. 7.—Cross-correlations of the ME light curves of observation B. The peak is not consistent with zero delay time and would imply that the variations in the 1–4 keV light curve precede the variations in the 4–9 keV light curve. However, this result is probably spurious; see text.

the background, which is then reflected in the background-subtracted source light curves. Indeed, if we cross-correlate either one of the source light curves in the two energy bands with the light curve of the background, we find a negative peak centered on zero time delay, which indicates an excess of background subtraction.

2.3. *Search for QPOs*

We reanalyzed the 1–9 keV ME light curves from the observations in Table 1 in order to carry out a detailed search for the QPOs with frequencies of ~ 1–2.5×10^{-3} Hz reported by PL. The 120 s binned light curve from each observation was divided into M consecutive intervals of ~ 1–2 hr duration, and the average power spectrum was calculated over the power spectra from individual intervals. This allowed us to reproduce approximately the frequency range and resolution used by PL in their analysis. Values of M equal to 23, 17, 8, 10, and 17 were used for observations J, C, I, A–F–G, and B–D, respectively. This method of analysis reduces by about one decade the low-frequency end of the power spectra, such that only marginal evidence is found for the increase toward low frequencies, which reflects the *red noise* variability of the source. In any case, to search for QPOs, we adopted a recently developed technique to detect significant power spectrum peaks even in the presence of "colored" noise components arising from the source variability (Israel & Stella 1996; Stella et al. 1995). The technique relies upon a suitable smoothing algorithm in order to model the continuum power spectrum components underlying any possible peak. By dividing the power spectrum by the smoothed spectrum, a flat (white noise–like) spectrum is produced, the statistical properties

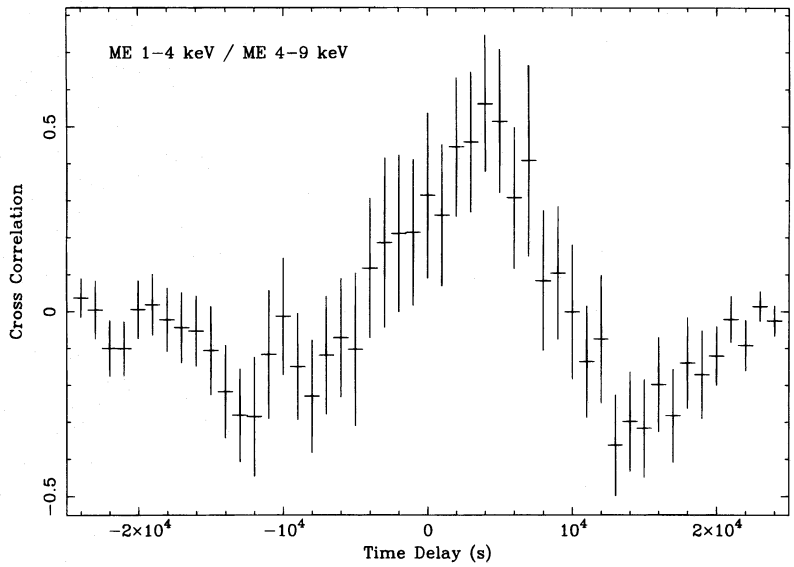

FIG. 8.—Cross-correlations of the ME light curves of observation G. The peak is not consistent with zero delay time and would imply that the variations in the 1–4 keV light curve precede the variations in the 4–9 keV light curve. However, this result is probably spurious; see text.

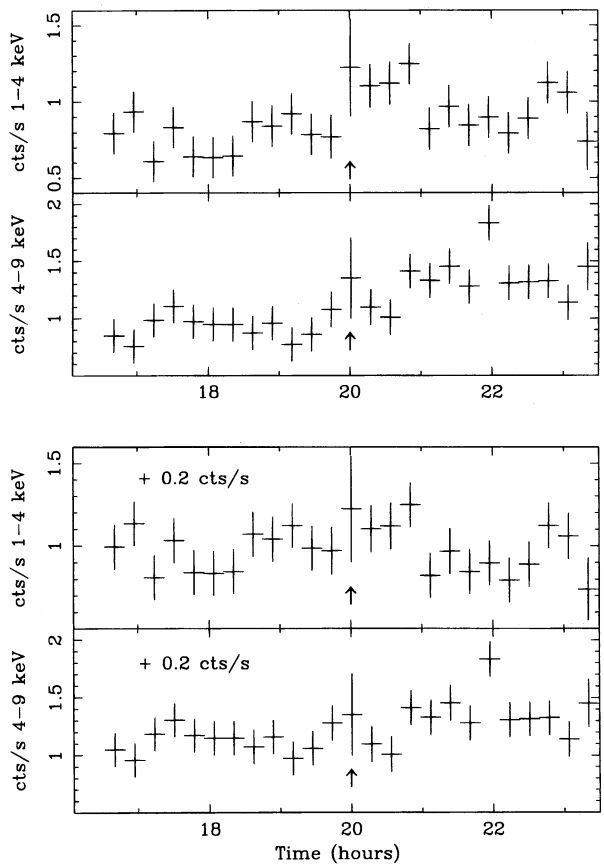

FIG. 9.—*Top:* ME light curves of observation G; the arrows show the array swap of the ME detector halves. *Bottom:* The same light curves after having added 0.2 counts s^{-1} to the two light curves before the array swap; the discontinuity due to the detector array swap is clearly reduced.

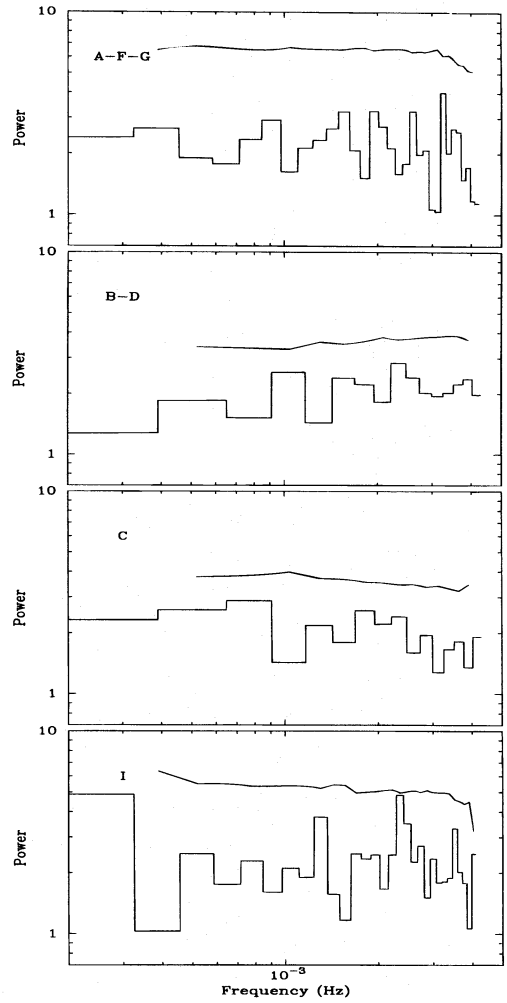

FIG. 10.—Power spectra from the *EXOSAT* ME 1–9 keV light curves of observations A–F–G (84/032, 85/173, and 85/186), B–D (84/062 and 85/062), C (84/193), and I (86/019) (*top to bottom*); the solid lines give the corresponding 95% confidence detection thresholds.

of which are worked out as the ratio of two random variables of know distribution, namely the power spectrum and the smoothed spectrum. A search for oscillations is then carried out by looking for peaks in the divided power spectrum that exceed a given detection threshold.

Selected average spectra and the corresponding 95% confidence detection thresholds are shown in Figure 10. No significant peaks exceeding the threshold were found in the frequency range $\sim 4 \times 10^{-4}$ to 4×10^{-3} Hz for any of the power spectra from observations C, B–D, A–F–G, J, and I. Observation J was also analyzed in different time intervals because of the possible malfunctioning of one of the ME detectors during the second half of the observation (see § 2.2). This was done by calculating a power spectrum for the source light curve and a power spectrum from the corresponding background light curve during each of the four array swap–free intervals in between the third array swap and the end of the observations. These power spectra and the corresponding 95% confidence detection thresholds are shown in Figure 11. Significant peaks are clearly detected in the second and fourth power spectra from the source at a frequency of about 1.8 and 2.6×10^{-3} Hz, respectively. It is very likely that these peaks were caused by some kind of quasi-periodic instability in the detector of the first half of the ME array that did not function properly during the second half of observation J. The LE light curves (0.05–2.0 keV), characterized by a poorer signal-to-noise ratio, were also searched for QPOs; only negative results were found.

Our results argue against the detection of QPOs in the X-ray flux of NGC 5548 reported by PL. The power spectrum technique used by PL involves averaging the logarithm of the power spectra from different intervals, thereby producing power estimates that approximately follow a Gaussian distribution (Papadakis & Lawrence 1993b). Model fitting can then be performed using standard least-squares techniques. The continuum power spectrum components are well fitted by a constant (representing the counting statistics noise) plus a power law (describing the source red noise). According to PL, the grouped power spectra from the three longest observations (C, I, and J) display a 95% significant QPO peak (as estimated through an *F*-test after the addition of a Gaussian to the model function). However, we have shown that the QPOs during observation J very likely arise from a detector problem.

PL devised also a test to evaluate the significance of power spectrum peaks from individual observations. The best-fit model (a power law plus a constant) is used to estimate the continuum components. The power spectrum is then divided by the best-fit model in order to produce a white noise power spectrum in which the presence of statistically significant peaks is tested. PL found, in three of five cases, a peak in the 1.1–2.4 $\times 10^{-3}$ Hz frequency range

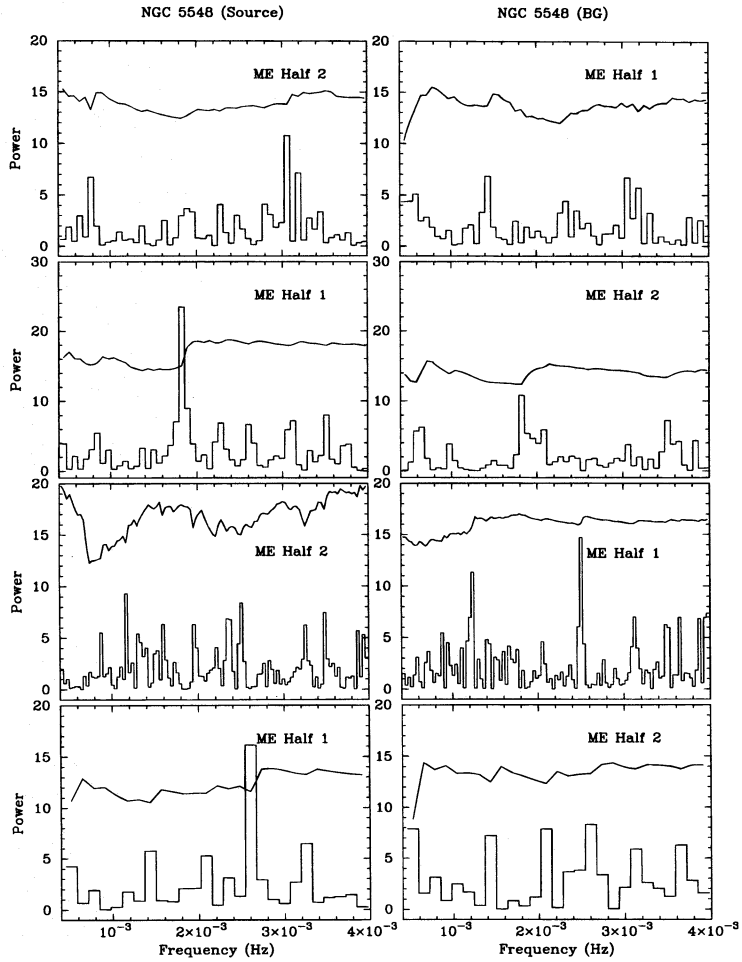

FIG. 11.—*EXOSAT* ME 1–9 keV power spectra of the ME light curves of NGC 5548 (*left*) and the background (*right*) during the second half of observation J. Each panel refers to an array swap–free interval, starting from the third array swap (see text for details). The ME array half used in each panel is indicated. The solid lines give the 95% confidence detection thresholds.

at a significance level of >95%. However, PL did not take into account the statistical uncertainties introduced into the divided power spectrum by the uncertainties in the best-fit model (as evidenced by the lack of any mention of them), therefore overestimating the significance of the peaks. To reassess this significance, we extracted the power spectra from Figure 1 of PL and fitted them with a constant, after excluding the power estimates corresponding to the peaks and the red noise. These constants, together with their 1 σ uncertainties on these averages, were then used to work out the distribution of the divided spectrum in a way that parallels the method of Israel & Stella (1996). Based on this distribution, the significance of the peaks in Figure 2 of PL was evaluated again. The divided power spectra of observations A–F–G (G3 in Table 1 of PL) and observation I are characterized by a peak with a significance of ~95% and ~88%, respectively. These values are lower than those worked out by PL (~98% and ~96%, respectively). The power spectrum of observation J, which formally contains the most significant peak, was disregarded because of the detector problem discussed above.

3. CONCLUSION

Our reanalysis of the CCFs of *EXOSAT* ME light curves of NGC 5548 does not confirm the claim of KB of a ~5000 s delay between the medium and soft X-ray variations. This was considered as a strong argument in favor of models in which medium-energy X-rays are produced by scattering of softer photons. Our results do not exclude this possibility. We note, however, that the 1990 *ROSAT* observations (Nandra et al. 1993) detected a variability pattern hardly consistent with very soft X-ray variations (0.1–0.4 keV) preceding the variations of somewhat harder X-rays (1–2.5 keV). This indicates the complexity of physical processes occurring in the source.

Our power spectrum analysis does not confirm the detection of QPOs in the mHz range reported by PL. In particular, we have shown that the only power spectrum peak with a significance of >95% most probably results from the malfunctioning of one ME detector. The argument of PL, according to which the black hole mass of NGC 5548 has an embarrassingly low value of a few hundred thousand solar masses, loses its validity.

While the results of this paper are essentially "negative," we hope that our work contributes illustrating subtle effects that may yield spurious results in the analysis of X-ray light curves from AGNs.

We thank an anonymous referee for her/his very useful comments and suggestions and A. N. Parmar for checking of the *EXOSAT* ME Observation Log Book and useful discussions on the ME *EXOSAT* data.

REFERENCES

Clavel, J., et al. 1991, ApJ, 366, 64
Clavel, J., et al. 1992, ApJ, 393,113
De Korte, P. A. J., et al. 1981, Space Sci. Rev., 30, 495
Done, C., Pounds, K. A., Nandra, K., & Fabian, A. 1995, MNRAS, 275, 417
Edelson, R. A., & Krolik, J. H. 1988, ApJ, 333, 646
The *EXOSAT* Database System: Available Databases. 1991, ESA TM-13 (Noordwijk: ESA Publication Division, ESTEC)
Giommi, P., Barr, P., Garilli, B., Gioia, I. M., Maccacaro, T., Maccagni, D., & Schild, R. E. 1987, ApJ, 322, 662
Grandi, P., Tagliaferri, G., Giommi, P., Barr, P., & Palumbo, G. C. 1992, ApJS, 82, 93
Green, A. R., McHardy, I. M., & Lehto, H. J. 1993, MNRAS, 265, 664
Haardt, F., & Maraschi, L. 1993, ApJ, 413, 507
Kaastra, J. S., & Barr, P. 1989, A&A, 226, 5 (KB)
Korista K. T., et al. 1995, ApJS, 97, 285
Israel, G. L. & Stella, L. 1996, ApJ, in press
Molendi, S., Maraschi, L., & Stella, L. 1992, MNRAS, 255, 27
Mushotzky, R. F., Done, C., & Pounds, K. A. 1993, ARA&A, 31, 717
Nandra, K., Pounds, K. A., Stewart, G. C., George, I. M., Hayashida, K., Makino, F., & Ohashi, T. 1991, MNRAS, 248, 760
Nandra, K., et al. 1993, MNRAS, 260, 504.
Papadakis, I. E., & Lawrence, A. 1993a, Nature, 361, 233 (PL)
———. 1993b, MNRAS, 261, 612
Parmar, A. N., & Izzo, C. 1986, *EXOSAT* Express, 16, 21
Stella, L., & Angelini L. 1992, in Data Analysis in Astronomy IV, ed. V. Di Gesù, L. Scarsi, R. Buccheri, P. Crane, M. C. Maccarone, & H. V. Zimmerman (New York: Plenum), 59
Stella, L., Arlandi, E., Tagliaferri, G., & Israel, G. L. 1995, in Time Series Analysis in Meterology and Astronomy, ed. S. Rao, in press
Tagliaferri, G., Stella, L., Maraschi, L., Treves, A., & Celotti, A. 1991, ApJ, 380, 78 (Paper I)
Turner, M. J. L., Smith, A., & Zimmermann, H. V. 1981, Space Sci. Rev., 30, 513
Walter, R., & Courvoisier, T. 1990, A&A, 233, 40
Walter, R., Courvoisier, T., Done, C., Maraschi, L., Pounds, K., & Urry, M. 1995, preprint
White, N. E., & Peacock, A. 1988, Mem. Soc. Astron. Italiana, 59, 7
Życki, P. T., Krolik, J. H., Zdziarski, A. A., & Kallman, T. R. 1994, ApJ, 437, 597